forests

MDPI

Article

Stomatal Limitation Is Able to Modulate Leaf Coloration Onset of Temperate Deciduous Tree

Hongying Yu [1,2], Guangsheng Zhou [1,2,3,*], Xiaomin Lv [1,2], Qijin He [4,*] and Mengzi Zhou [1,2]

1 State Key Laboratory of Severe Weather, Chinese Academy of Meteorological Sciences, Beijing 100081, China; woyuhying@163.com (H.Y.); lvxm@cma.gov.cn (X.L.); zhoumengzi@cma.gov.cn (M.Z.)
2 Hebei Gucheng Agricultural Meteorology National Observation and Research Station, Baoding 072656, China
3 Collaborative Innovation Center on Forecast Meteorological Disaster Warning and Assessment, Nanjing University of Information Science & Technology, Nanjing 210044, China
4 College of Resources and Environmental Sciences, China Agricultural University, Beijing 100193, China
* Correspondence: zhougs@cma.gov.cn (G.Z.); heqijin@cau.edu.cn (Q.H.)

Abstract: Autumn phenology, determined mainly by temperature and photoperiod, is essential for ecosystem carbon sequestration. Usually, the variations in the maximum rate of Rubisco (V_{cmax}) and the maximum rate of ribulose-bisphosphate regeneration (J_{max}) are taken as the mechanism regulating the seasonal pattern of photosynthetic rates and autumn phenology. In this study, we used *Quercus mongolicus* seedlings as an example to examine the photosynthetically physiological mechanism of leaf coloration onset (LCO) responding to different warming and photoperiod treatments based on experimental data acquired from large artificial climate simulation chambers. The results indicated that: (1) LCO and the net CO_2 assimilation rate (P_n), transpiration rate (T_r), stomatal conductance (G_s), V_{cmax}, and J_{max} of *Quercus mongolicus* seedlings were significantly affected by the changes of photoperiod. (2) LCO was significantly correlated only with the P_n approach, supporting the view that leaf senescence is the result of a trade-off between nutrient resorption and reserves. (3) The major variation in stomatal conductance (G_s) is the mechanism by which photoperiod regulates the seasonal pattern of photosynthetic rates, implying that both limitations of stomatal and photosynthetical capacity (V_{cmax} and J_{max}, non-stomatal limitation) are able to modulate LCO. Our study riches the knowledge of phenology and provides a reference for phenological modelling and ecosystem carbon estimation.

Keywords: leaf senescence; regulation mechanism; stomatal limitation; photosynthetical capacity; temperate deciduous tree

check for updates

Citation: Yu, H.; Zhou, G.; Lv, X.; He, Q.; Zhou, M. Stomatal Limitation Is Able to Modulate Leaf Coloration Onset of Temperate Deciduous Tree. *Forests* **2022**, *13*, 1099. https://doi.org/10.3390/f13071099

Received: 13 June 2022
Accepted: 11 July 2022
Published: 13 July 2022

Publisher's Note: MDPI stays neutral with regard to jurisdictional claims in published maps and institutional affiliations.

Copyright: © 2022 by the authors. Licensee MDPI, Basel, Switzerland. This article is an open access article distributed under the terms and conditions of the Creative Commons Attribution (CC BY) license (https://creativecommons.org/licenses/by/4.0/).

1. Introduction

Plant phenology, particularly the length of the growing season (from leaf expansion to leaf coloring), is closely related to vegetation productivity and carbon sequestration [1–4]. Plant phenology is sensitive to climate change and has already changed because of the increase in global warming [5–7]. Evidence from many regions worldwide demonstrates that climate change has advanced spring phenology, delayed autumn phenology, and induced a prolonged growing season [8–11]. Autumn phenology (i.e., leaf coloring and leaf drop) may affect individual plant reproductive ability and the length of the growing season, which are crucial to ecosystem net productivity and the carbon cycle [12–15]. Phenological changes over the Northern Hemisphere suggest that the extension of the growing season in recent decades is due to the postponed autumn phenology rather than advanced spring phenology [16]. A flux study from 22 forest sites in North America and Europe also showed that changes in ecosystem net productivity can be largely explained by autumn phenology variation, and autumn phenology has a greater impact than spring phenology [17]. These results highlight that autumn phenology influences ecosystem carbon sequestration more than spring phenology does. However, research on autumn phenology and its mechanism is far less than spring phenology.

Temperature and photoperiod are the two major limiting factors of autumn phenology [15,18]. Reports have indicated that leaf phenology is particularly sensitive to temperature; warming can delay leaf senescence and postpone the end of the growth season [19–22]. Because of the regulation of photoperiod, another factor driving plant phenology, leaf senescence in some plants occurs almost on the same day each year [2,23]. A study of the Qinghai Tibet Plateau found that leaf senescence of all alien species is mainly caused by the shortening of photoperiod, not the location [20]. Effects of temperature and photoperiod on leaf senescence may be attributed to a trade-off between carbon and nitrogen metabolism. Plants choose the best leaf senescence time to simultaneously extend the growing season to increase carbon reserves, reduce the risk of low-temperature damage, and maximize nitrogen recovery before frost [24–26]. Zani et al. [27] found that increased seasonal productivity could be an influential driver of earlier leaf senescence in temperate deciduous trees because elevated carbon capture shortens the productive season. The physiological processes and mechanisms underlying the effects of photoperiod and temperature on autumn phenology are unclear.

Quercus *mongolicus* is one of the dominant tree species in East Asian broad-leaved forests; it protects from the wind, conserves water, and prevents fire and ecological development; it has been observed in Russia, China, the Korean Peninsula, and Japan [28]. As a light-favored species, light conditions play a vital role in the morphology, photosynthesis, biomass, and phenology of *Quercus mongolicus* [29]. With global climate warming, the distribution of *Quercus mongolicus* will expand, leading to changes in temperature and photoperiod. Based on this background, studying the influence of temperature and photoperiod on the autumn phenology of *Quercus mongolicus* and the associated mechanism is a matter of urgency. We performed a simulated experiment with a large artificial climate chamber to study the effects and interactions of warming and photoperiod on *Quercus mongolicus* seedling (3-year-old) leaf coloration onset (LCO), explored the underlying physiological mechanism from the viewpoint of photosynthetic physiology, and provided a basis for the development of phenological models of *Quercus mongolicus*. We hypothesized that (1) photoperiod and warming affect LCO by influencing photosynthesis indirectly; (2) there is a critical period for photosynthesis to adjust the LCO; (3) photosynthesis regulates the LCO by the maximum rate of Rubisco (V_{cmax}) and the maximum rate of ribulose-bisphosphate regeneration (J_{max}).

2. Materials and Methods

2.1. Experimental Design

2.1.1. Study Site and Climate Chambers

This experiment was conducted at the Hebei Gucheng Agricultural Meteorology National Observation and Research Station, Hebei Province, China (39′08″ N, 115′40″ E, 15.2 m a.s.l.). Three large artificial climate chambers were used to simulate and control the growth conditions. The chamber could be artificially warmed/cooled by a centralized heating/cooling system which could ensure different levels of continuous (day and night) warming/cooling above/below fluctuating ambient air temperature. Each chamber was assigned to one temperature treatment and separated into six cubicles by wooden boards and opaque curtains to achieve different photoperiod treatments (Figure 1). Each cubicle of each chamber had one group of sodium lamps and accommodated 2 saplings; we switched the lamps and curtains at different times to obtain three photoperiod treatments.



Figure 1. The large artificial climate chamber photos showing (**A**) the three artificial climate chambers, (**B**) six cubicles of each chamber separated by wooden boards and opaque curtains, and (**C**) a view of the cubicle and the lamps in it.

2.1.2. Tree Material

We selected 3-year-old *Quercus mongolicus* seedlings with similar growth status from the forest farm of Baiquan County, Qiqihar City, Heilongjiang Province, China. Seedlings were transplanted to plastic pots (20 cm in diameter, 20 cm in height) filled with soil from their original location (1 plant per pot). Seedlings were moved into large artificial climate chambers and maintained in the simulated environment of their original place for 15 d. Temperature and photoperiod control experiments were started in April 2019.

2.1.3. Treatments and Environment Controls

We set up three temperature treatments and three photoperiod treatments, resulting in nine treatments. The temperature treatments were as follows: control (the mean corresponding month temperature of the original place of *Quercus mongolicus* seedlings from 1989 to 2018, T1) (Table 1); 1.5 °C warming (T2); 2.0 °C warming (T3), and the temperature was set at the first day of each month during the experiment. Photoperiod treatments were as follows: 18 h photoperiod (long photoperiod, L1); 14 h photoperiod, the average photoperiod of the original place from 1989 to 2018 (control, L2); 10 h photoperiod (short photoperiod, L3). Each treatment had four replicates, and each replicate contained one seedling. Temperature and air relative humidity (the mean corresponding month air relative humidity of the original place of *Quercus mongolicus* seedlings from 1989 to 2018) (Table 1) were set on the first day of each month and automatically controlled by the large artificial climate chamber. The concentration of CO_2 was set to the atmospheric CO_2 concentration (400 $\pm$ 20 μmol/mol). To ensure seedling survival, the seedlings were watered every 3 d with the amount calculated by the mean corresponding month precipitation of the original place (Table 1). We did not apply any fertilizer during the experiment.

Table 1. Simulated climatic parameters of the control group during the experiment.

Month	Temperature (°C)	Relative Humidity (%)	Precipitation (mm)	Irrigation Amount (mL)
April	5.65	50.94	19.51	55
May	14.02	51.41	37.64	107
June	19.96	65.16	87.04	247
July	22.33	76.87	155.24	440
August	20.28	78.68	113.22	321
September	13.61	69.75	54.45	154
October	4.45	61.76	20.16	57

2.2. Phenology Observation

According to Wan and Liu [30], LCO was defined as the date when the first leaves had an autumn color. Observations were conducted every 2 d at 2:00 p.m., and LCO was recorded.

2.3. Leaf Gas Exchange Parameters and CO_2 Response Curve Measurements

The net CO_2 assimilation rate (P_n), transpiration rate (T_r), stomatal conductance (G_s), intercellular CO_2 concentration (C_i), and C_i/C_a ratio (C_i/C_a) were measured from 8:30 a.m. to 3:30 p.m. on 22 May, 27 June, 18 July, 1 August, and LCO in 2019, using an open gas exchange system (LI-6400, Li-COR Inc., Lincoln, NE) with a leaf chamber fluorometer attachment (LI6400-40, LCF). Three plants from each treatment were selected, and the first full-spread leaf at the top of the chosen plant was used for testing. The concentration of CO_2 was fixed at 400 $\mu mol \cdot mol^{-1}$, temperature was set at 25 °C, photosynthetic photon flux density (*PPFD*) was applied with saturating irradiance (1500 $\mu mol \cdot m^{-2} \cdot s^{-1}$) supplied via a red-blue LED, and leaves were acclimated under this environmental condition for 10 min.

Measurements were made on the same leaves under a saturated *PPFD* of 1500 $\mu mol \cdot m^{-2} \cdot s^{-1}$ at 25 °C on 1 August 2019. The CO_2 concentration gradient for the A/Ci curves was 400, 300, 200, 100, 0, 400, 400, 600, 800, 1000, 1500, 1800, and 2000 $\mu mol \cdot mol^{-1}$. Leaves are able to maintain a steady state quickly when external CO_2 concentration changes (even shorter than 1s) [31,32]. We set minimum wait time at 60 s after each CO_2 concentration change, which is enough for leaf to adapt, and then system will check stability to see if it can log. Detailed steps were provided in the Supplementary Information.

Data were recorded when system stability was met: (1) the standard deviation of the net CO_2 assimilation rate (P_n) in 20 s was <0.5; (2) the standard deviation of stomatal conductance (G_s) in 20 s was <0.1; (3) the rate of change of P_n was <0.1 per minute; and (4) the rate of change of G_s was <0.05 per minute. We matched before each recording to minimize offsets between the sample and reference analyzers and improve the accuracy of the measurements. The maximum rate of Rubisco (V_{cmax}) and maximum rate of ribulose-bisphosphate regeneration (J_{max}) were calculated using photosynthesis software (Li-COR Inc., Lincoln, NE, USA).

2.4. Leaf Chlorophyll Content and Water Content Measurements

The contents of leaf chlorophyll and water were measured at the same leaf used to measure leaf gas exchange parameters and the CO_2 response curve. Leaf chlorophyll content was measured by a chlorophyll content meter (CCM-300, Opti-Sciences Inc., Hudson, NH, USA).

Leaves were quickly separated and weighed after all the other measurements, to avoid water loss, and then placed in an oven at 80 °C for at least 48 h to a constant dry weight. The leaf water content (LWC) was calculated by using the following formula [33,34].

$$LWC = \frac{LFW - LDM}{LFW} \times 100\%$$

where LFW and LDM indicate leaf fresh weight and leaf dry mass (g), respectively.

2.5. Statistical Analysis

A two-way ANOVA with LSD tests was used to test the effects of temperature, photoperiod, and their interaction on P_n, T_r, G_s, C_i, and C_i/C_a at different periods; LCO; V_{cmax}; J_{max}; chlorophyll content; and the LWC of *Quercus mongolicus* seedlings. Pearson's correlation analysis was used to explore the correlation between the P_n of different periods and LCO. All analyses were performed by SPSS 21.0 (IBM, Armonk, NY, USA). The structural equation model (SEM) conducted by Amos 21.0 (Amos Development, Spring House, PA, USA) was used to analyze pathways that may explain how temperature and photoperiod regulate LCO. The statistical significance level of all analyses was set at $p < 0.05$ unless stated otherwise.

3. Results

3.1. LCO under Different Temperature and Photoperiod Treatments

Photoperiod had a significant effect on LCO of *Quercus mongolicus* seedlings ($p < 0.01$); LCO of the L3 (short photoperiod, 10 h) was significantly later than that of L2 (control, 14 h) and L1 (long photoperiod, 18 h) ($p < 0.05$, Figure 2). Temperature and its interaction with photoperiod had no significant effects. Only under L1 treatment, LCO of T3 was significantly later than that of T1. The average LCO of the L1, L2, and L3 treatments were 224.3 d, 228.8 d, 236.9 d, respectively.

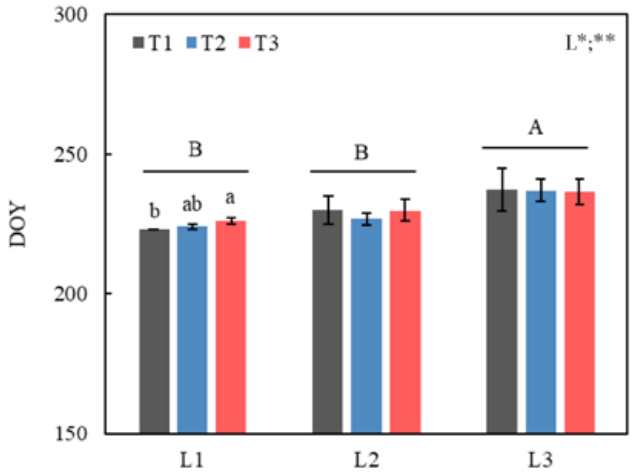


Figure 2. Changes in leaf coloration onset (LCO) of *Quercus mongolicus* seedlings under the temperature and photoperiod treatments. Error bars represent means ± SE (n = 4). DOY represents day of year; T1 represents control; T2 represents 1.5 °C warming; T3 represents 2.0 °C warming; L1 represents 18 h photoperiod (long photoperiod), L2 represents 14 h photoperiod (control), and L3 represents 10 h photoperiod (short photoperiod). The different uppercase letters show significant differences among photoperiod treatments ($p < 0.05$), and the lowercase letters show significant differences among temperature treatments ($p < 0.05$). * and ** were used to indicate significant differences in temperature (T) and photoperiod (L) and their interaction effect at $p < 0.05$ and $p < 0.01$, respectively.

3.2. Leaf Gas Exchange Parameters under Different Temperature and Photoperiod Treatments

The photoperiod significantly changed P_n from July to LCO, T_r from May to LCO, and G_s from June to LCO ($p < 0.05$) and reached an extremely significant level in August ($p < 0.01$) (Table 2, Figure 3). For C_i and C_i/C_a, the photoperiod only significantly affected them in May ($p < 0.01$) (Table 2). Temperature had significant effects on P_n in May and July, T_r from May to July, and G_s in May and June (Table 2). The interaction between temperature and photoperiod affected the P_n of LCO, T_r in June and July, and G_s in June (Table 2).

Table 2. Effects of photoperiod (L), temperature (T), and their interaction on leaf gas exchange parameters of *Quercus mongolicus* seedlings.

	Month	L			T			L × T		
		df	**F**	***P***	**df**	**F**	***P***	**df**	**F**	***P***
P_n	May	2	0.49	0.62	2	4.24	**<0.05**	4	0.33	0.86
	June	2	2.52	0.14	2	2.58	0.13	4	1.54	0.27
	July	2	3.86	**<0.05**	2	5.23	**<0.05**	4	2.44	0.10
	August	2	33.39	**<0.01**	2	1.26	0.31	4	1.51	0.25
	LCO	2	4.19	**<0.05**	2	1.84	0.20	4	4.06	**<0.05**
G_s	May	2	1.07	0.36	2	8.45	**<0.01**	4	1.04	0.42
	June	2	7.74	**<0.05**	2	9.23	**<0.01**	4	4.79	**<0.05**
	July	2	4.96	**<0.05**	2	2.53	0.12	4	1.85	0.18
	August	2	23.86	**<0.01**	2	0.11	0.90	4	1.30	0.32
	LCO	2	4.13	**<0.05**	2	1.24	0.32	4	2.62	0.09
C_i	May	2	9.53	**<0.01**	2	3.36	0.06	4	0.45	0.77
	June	2	0.03	0.97	2	1.55	0.26	4	0.34	0.85
	July	2	2.97	0.08	2	1.71	0.22	4	3.02	0.05
	August	2	0.84	0.45	2	0.56	0.58	4	1.39	0.29
	LCO	2	0.38	0.69	2	0.06	0.94	4	0.16	0.95
C_i/C_a	May	2	9.58	**<0.01**	2	3.45	0.06	4	0.45	0.77
	June	2	0.05	0.95	2	1.67	0.24	4	0.37	0.82
	July	2	2.94	0.09	2	1.69	0.22	4	3.02	0.06
	August	2	0.82	0.46	2	0.50	0.62	4	1.40	0.28
	LCO	2	0.40	0.68	2	0.05	0.95	4	0.15	0.96
T_r	May	2	4.84	**<0.05**	2	13.18	**<0.01**	4	2.30	0.10
	June	2	22.35	**<0.01**	2	15.48	**<0.01**	4	7.49	**<0.01**
	July	2	11.66	**<0.01**	2	4.37	**<0.05**	4	3.74	**<0.05**
	August	2	18.88	**<0.01**	2	0.07	0.93	4	1.48	0.26
	LCO	2	5.31	**<0.05**	2	1.01	0.39	4	1.94	0.17

Notes: P_n represents the net CO_2 assimilation rate; G_s represents stomatal conductance; C_i represents intercellular CO_2 concentration; C_i/C_a represents C_i/C_a ratio; T_r represents transpiration rate; LCO represents leaf coloration onset. The bold data indicate significant differences at $p < 0.05$ and $p < 0.01$, respectively.

3.3. Regulation Mechanisms of Temperature and Photoperiod on LCO

As shown, only P_n in August (near LCO) was significantly correlated with LCO ($R^2 = 0.65$, $p < 0.01$) (Figure 4); therefore, the time near LCO may be the key regulating LCO variations. The photoperiod significantly changed the maximum rate of Rubisco (V_{cmax}) and the maximum rate of ribulose-bisphosphate regeneration (J_{max}) near the time of LCO, whereas temperature and its interaction with photoperiod had no significant effect ($p < 0.05$, Table 3). Both leaf chlorophyll content and water content showed no significant response to photoperiod, temperature, or their interaction (Table 3).

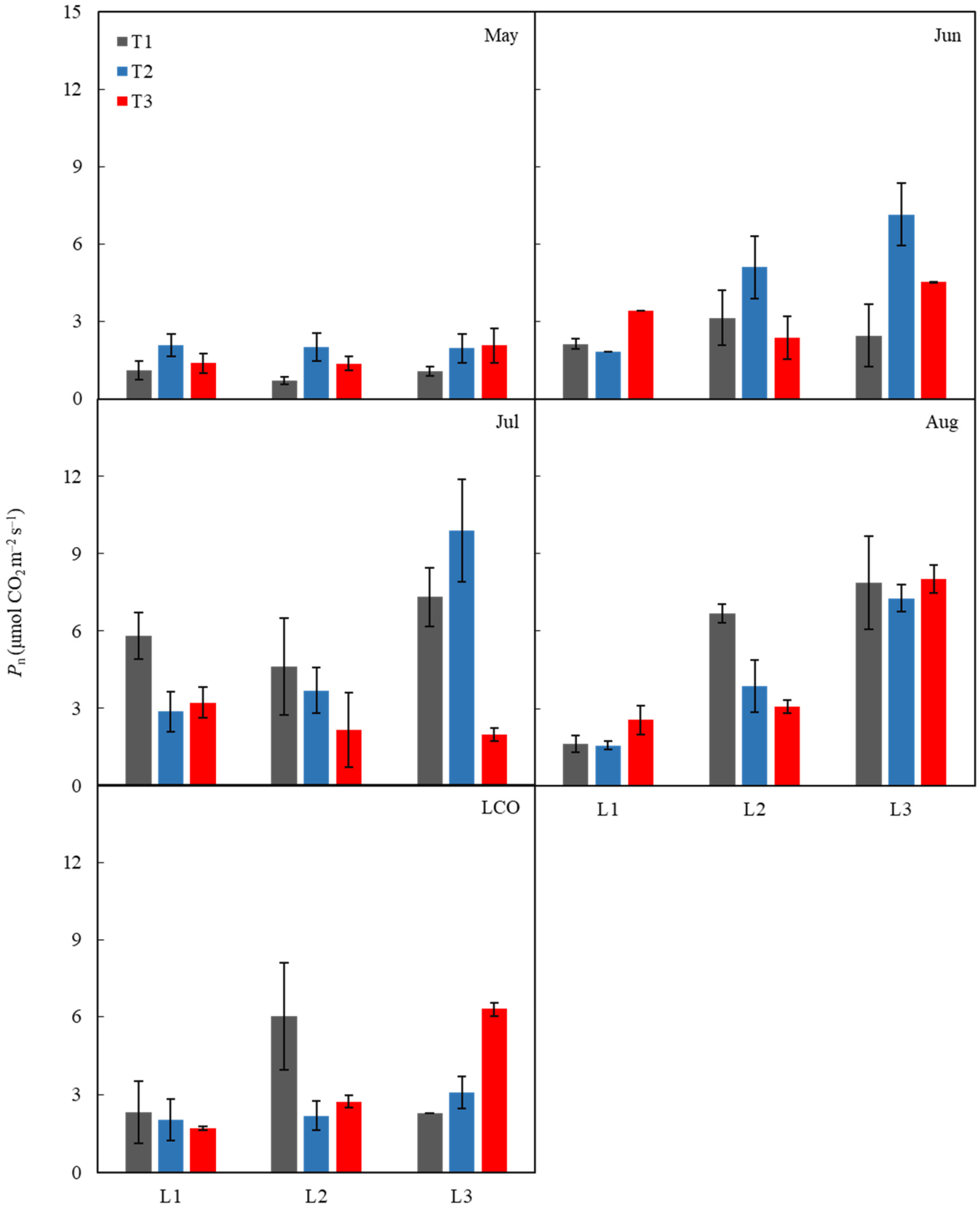


Figure 3. Changes in the net CO_2 assimilation rate (P_n) of different periods under the temperature and photoperiod treatments. Error bars represent means ± SE (n = 3). T1 represents control; T2 represents 1.5 °C warming; T3 represents 2.0 °C warming; L1 represents 18 h photoperiod (long photoperiod), L2 represents 14 h photoperiod (control), and L3 represents 10 h photoperiod (short photoperiod).

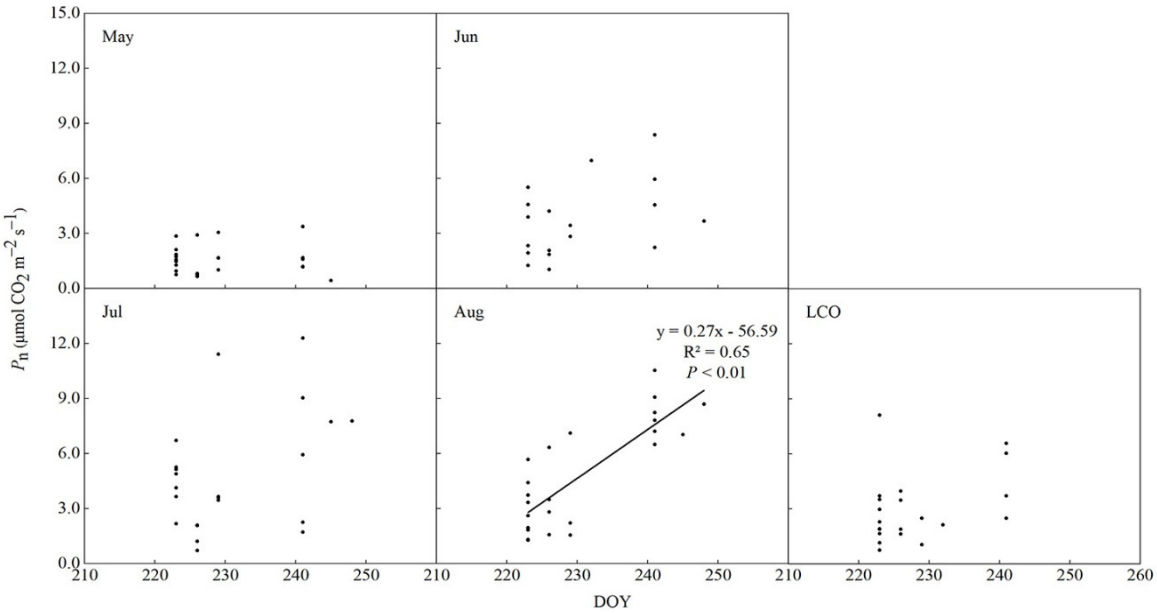


Figure 4. Relationships between P_n of different periods and LCO of *Quercus mongolicus* seedlings.

Table 3. Effects of photoperiod (L), temperature (T), and their interaction on photosynthetic parameters, leaf chlorophyll content, and water content near LCO.

	L			T			L × T		
	df	**F**	***P***	**df**	**F**	***P***	**df**	**F**	***P***
V_{cmax}	2	5.15	**<0.05**	2	0.82	0.46	4	0.98	0.45
J_{max}	2	5.30	**<0.05**	2	0.93	0.42	4	0.03	1.00
Chl	2	1.26	0.31	2	0.37	0.70	4	0.35	0.84
LWC	2	2.74	0.09	2	1.97	0.17	4	0.37	0.83

Notes: V_{cmax} and J_{max} represent the maximum rate of Rubisco and maximum rate of ribulose-bisphosphate regeneration, respectively. Chl represents the chlorophyll content. LWC represents the leaf water content. The bold data indicate significant differences at $p < 0.05$ and $p < 0.01$, respectively.

The structural equation model (SEM) results indicated that temperature had no significant direct or indirect impact on photosynthetic characteristics and LCO. Photoperiod had a significant direct impact on G_s, V_{cmax}, and J_{max} and explained 66% of the variation in G_s. Among the photosynthetic characteristics, G_s had a significant direct impact on P_n, with a standardized path coefficient of 0.85 (Figure 5). In summary, photoperiod affected P_n near LCO indirectly by changing G_s and regulating LCO (Figure 5). The model explained 64% of the variation in LCO (Figure 5).

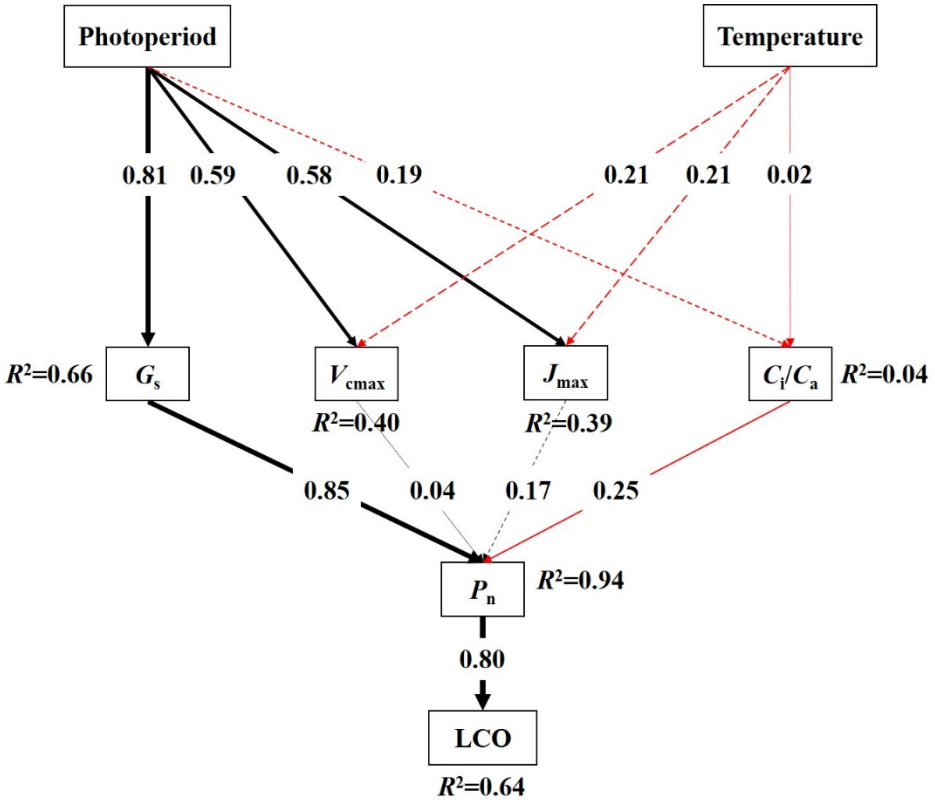


Figure 5. Structural equation model (SEM) analysis of the effects of photoperiod and temperature on LCO. Square boxes indicate variables in the model. Results of model fitting: $\chi^2 = 4.00$, $p = 0.95$, df = 10, and $n = 23$. Black and red arrows denote the positive and negative correlation pathways, respectively. Arrow width indicates relationship strength. Solid and dashed lines represent significant ($p < 0.05$) and nonsignificant ($p > 0.05$) pathways, respectively. The number associated with the arrow represents standardized path coefficients, and R^2 values indicate the proportion of the variation explained for each dependent variable in the model.

4. Discussion

In deciduous plants, leaf senescence is the transition between the active and dormant periods. Plants complete nutrient resorption before leaf drop to provide nutrients for the construction of new leaves in the following year [25]. The duration of leaf senescence results from a trade-off between nitrogen and carbon requirements. Trees shorten their growing season and decrease photosynthetic proficiency by triggering senescence early to efficiently remobilize nitrogen. By contrast, trees that are senescent too late can obtain more photosynthates but are threatened by nitrogen loss in leaves, owing to frost damage and the reduction of nutrient support for the growth of leaves in the next season [23,35,36]. Temperature and photoperiod are the two main climatic factors affecting autumn phenology [37–39]. Photoperiod is a signal that predicts the arrival of cold and frost, and temperature can predict warmth [25,40].

In this study, the temperature had no significant effect on LCO. Studies have illustrated that autumn phenology is delayed as temperatures increase [41–44]; nonetheless, different species respond differently to temperature. Temperature exerted various influences on leaf senescence in four deciduous forest species (*Liquidambar styraciflua*, *Quercus rubra*, *Populus grandidentata*, *Betula alleghaniensis*) and affected *Quercus* the least [45]. Morin et al. [46] also found different responses of leaf senescence to temperature in two deciduous species (*Quercus robur*, *Quercus pubescens*). Similarly, autumn phenology from 13 observation sites in Finnish Lapland showed no trends or relationships with climatic conditions [47]. In this study, the interaction effect of photoperiod and temperature on LCO of *Quercus mongolicus* seedlings was not significant. This was not in line with previous results, which may be caused by spatial and interspecific difference. Delpierre et al. [38] proposed a

photoperiod-sensitive cold-degree day summation model to simulate leaf coloring and obtained a good result. Lang et al. [20] reported the coupling effect of photoperiod shortening and temperature decreases on leaf senescence. The start of leaf senescence was 61.2% controlled by photoperiod shortening, and 38.8% controlled by daily minimum temperature decrease, particularly for the native species. In all exotic species, leaf senescence start was triggered by photoperiod shortening. They concluded that the response of leaf senescence to photoperiod and temperature varied by species and space, as confirmed by Tanino et al. [48].

In our study, photoperiod changed LCO significantly; the short photoperiod postponed LCO, and long photoperiod advanced it, which is inconsistent with results in the literature. A general consensus is that photoperiod drives leaf coloring and senescence. Experimental and observational data have proved that the senescence process started around the same date, and a vast majority of studies have demonstrated that the shortening photoperiod is a driver of leaf coloring and senescence [20,23,35,49]. However, our results support the view that leaf senescence is the result of a trade-off between nutrient resorption and reserves. Plants postponed LCO to compensate for the enormous insufficiency in photosynthetic time under the condition of a long-time short photoperiod relative to a long-photoperiod and maximum carbon accumulation. During our experiment, P_n of the short-photoperiod treatment was gradually higher than that of the control and long-photoperiod treatments and reached a significant level near LCO, which may be a compensatory measure by which plants can shift from resource assimilation to remobilization as soon as possible. Furthermore, leaf senescence relies heavily on photosynthesis to provide the energy it demands. Quercus *mongolicus* seedlings in short-photoperiod treatments for long periods therefore need to defer LCO and increase P_n to ensure the energy required for leaf senescence [23,35].

We found that the P_n near LCO had a close relationship with LCO, and the photoperiod adjusted the P_n near LCO indirectly by changing G_s and modulating LCO. Studies have shown that the photoperiod is pivotal in plant photosynthesis [50,51]. Photoperiod explains the major variation in V_{cmax} and J_{max} across 23 tree species and is the mechanism by which photoperiod regulates the seasonal pattern of photosynthetic rates [52]. In *Gingko biloba*, photoperiod is highly synchronized and correlated with V_{cmax} [53]. Contrary to their results, our study supports that even photoperiod had significant direct effects on G_s, V_{cmax}, and J_{max}, which mainly controlled P_n by altering G_s. The interspecific difference and the seedlings we used instead of mature trees may be responsible for this difference.

To be noted, the seedlings in pots usually have distinctly different biomass allocation, carbohydrate dynamics and attendant variation in carbon assimilation mechanisms compared to massive adult trees in natural systems. The controlled pot studies, however, are necessary to improve the understanding of the process and mechanism of forest ecosystems from seedlings to adult trees. There are uncertainties associated with jumping from the pot to the forest scale, and the results from the controlled pot studies could not directly come to generalizing to the trees. In order to realize the results from manipulated experiment to generalizing to the trees, in-situ control experimental research should be strengthened in the future, although it has high costs and it is difficult to achieve multi-environmental factor control.

5. Conclusions

We conducted an experiment with three temperature and three photoperiod treatments and found that photoperiod was the driver of LCO in *Quercus mongolicus* seedlings, but not temperature or their interaction. The *Quercus mongolicus* seedlings that suffered in a short photoperiod for a long time postponed LCO significantly, and seedlings of the long-photoperiod treatments advanced their LCO. Seedlings in the short-photoperiod treatments had higher P_n than the other two treatments, especially at the date near LCO. The later LCO and higher P_n of the short-photoperiod seedlings may compensate for insufficiency in photosynthetic time and maximize carbon accumulation before leaf senescence, supporting

the view that leaf senescence is a trade-off between plant nutrient resorption and reserves from another insight. The close relationship between P_n near LCO and LCO suggests that P_n is the key driver of LCO, and the pathway of the photoperiod regulation of LCO is that photoperiod changes G_s near LCO, which indirectly affects P_n.

Supplementary Materials: The following supporting information can be downloaded at: https://www.mdpi.com/article/10.3390/f13071099/s1.

Author Contributions: Conceptualization, G.Z. and Q.H.; methodology, M.Z., G.Z. and Q.H.; software, H.Y.; formal analysis, H.Y.; investigation, H.Y., X.L. and M.Z.; resources, X.L. and M.Z.; writing—original draft, H.Y.; writing—review & editing, M.Z., G.Z. and Q.H.; visualization, H.Y.; supervision, G.Z.; project administration, G.Z. and Q.H.; funding acquisition, G.Z. and Q.H. All authors have read and agreed to the published version of the manuscript.

Funding: This study is supported by the National Key Research and Development Program of China (No. 2018YFD0606103), the National Natural Science Foundation of China (No. 4213000565), and the Basic Research Fund of Chinese Academy of Meteorological Sciences (2020Z004).

Institutional Review Board Statement: Not applicable.

Informed Consent Statement: Not applicable.

Data Availability Statement: Not applicable.

Acknowledgments: The authors wish to thank Mingxin, Hu, Siqi Wang, Shiya Zhang, Wenjie Gu, Ruochen Li, Xingyang Song Erhua Liu, and Huailin Zhou for their assistance in the manipulation experiment.

Conflicts of Interest: The authors declare that they have no known competing financial interests or personal relationships that could have appeared to influence the work reported in this paper.

References

1. Ge, Q.; Wang, H.; Rutishauser, T.; Dai, J. Phenological response to climate change in China: A meta-analysis. *Glob. Chang. Biol.* **2015**, *21*, 265–274. [CrossRef]
2. Piao, S.; Liu, Q.; Chen, A.; Janssens, I.A.; Fu, Y.; Dai, J.; Liu, L.; Lian, X.; Shen, M.; Zhu, X. Plant phenology and global climate change: Current progresses and challenges. *Glob. Chang. Biol.* **2019**, *25*, 1922–1940. [CrossRef] [PubMed]
3. Wang, S.Q.; Zhou, G.S.; Zhou, M.Z.; Lü, X.M.; Zhou, L.; Ji, Y.H. Photosynthetically physiological mechanism of *Stipa krylovii* withered and yellow phenology response to precipitation under the background of warming. *J. Appl. Ecol.* **2021**, *32*, 845–852. [CrossRef]
4. Zhou, L.; Wang, Y.; Jia, Q.; Zhou, G. Increasing temperature shortened the carbon uptake period and decreased the cumulative net ecosystem productivity in a maize cropland in Northeast China. *Field Crop Res.* **2021**, *267*, 108150. [CrossRef]
5. Steinaker, D.F.; Wilson, S.D. Phenology of fine roots and leaves in forest and grassland. *J. Ecol.* **2008**, *96*, 1222–1229. [CrossRef]
6. Huang, L.; Koubek, T.; Weiser, M.; Herben, T.; Cornelissen, H. Environmental drivers and phylogenetic constraints of growth phenologies across a large set of herbaceous species. *J. Ecol.* **2018**, *106*, 1621–1633. [CrossRef]
7. Berra, E.F.; Gaulton, R. Remote sensing of temperate and boreal forest phenology: A review of progress, challenges and opportunities in the intercomparison of in-situ and satellite phenological metrics. *Forest Ecol. Manag.* **2021**, *480*, 118663. [CrossRef]
8. Menzel, A. Trends in phenological phases in Europe between 1951 and 1996. *Int. J. Biometeorol.* **2000**, *44*, 76–81. [CrossRef]
9. Cleland, E.E.; Allen, J.M.; Crimmins, T.M.; Dunne, J.A.; Pau, S.; Travers, S.E.; Zavaleta, E.S.; Wolkovich, E.M. Phenological tracking enables positive species responses to climate change. *Ecology* **2012**, *93*, 1765–1771. [CrossRef]
10. Svystun, T.; Lundströmer, J.; Berlin, M.; Westin, J.; Jönsson, A.M. Model analysis of temperature impact on the Norway spruce provenance specific bud burst and associated risk of frost damage. *Forest Ecol. Manag.* **2021**, *493*, 119252. [CrossRef]
11. Zhang, R.; Wang, F.; Zheng, J.; Lin, J.; Hänninen, H.; Wu, J. Chilling accumulation and photoperiod regulate rest break and bud burst in five subtropical tree species. *Forest Ecol. Manag.* **2021**, *485*, 118813. [CrossRef]
12. Liu, L.; Zhang, X.; Yu, Y.; Donnelly, A. Detecting spatiotemporal changes of peak foliage coloration in deciduous and mixedforests across the Central and Eastern United States. *Environ. Res. Lett.* **2017**, *12*, 024013. [CrossRef]
13. Li, P.; Peng, C.; Wang, M.; Luo, Y.; Li, M.; Zhang, K.; Zhang, D.; Zhu, Q. Dynamics of vegetation autumn phenology and its response to multiple environmental factors from 1982 to 2012 on Qinghai-Tibetan Plateau in China. *Sci. Total Environ.* **2018**, *637–638*, 855–864. [CrossRef] [PubMed]
14. Li, P.; Zhu, Q.; Peng, C.; Zhang, J.; Wang, M.; Zhang, J.; Ding, J.; Zhou, X. Change in autumn vegetation phenology and the climate controls from 1982 to 2012 on the Qinghai–Tibet Plateau. *Front. Plant Sci.* **2020**, *10*, 1677. [CrossRef]
15. Zhang, S.; Dai, J.; Ge, Q. Responses of autumn phenology to climate change and the correlations of plant hormone regulation. *Sci. Rep.* **2020**, *10*, 9039. [CrossRef]

16. Jeong, S.J.; Ho, C.H.; Gim, H.J.; Brown, M.E. Phenology shifts at start vs. end of growing season in temperate vegetation over the Northern Hemisphere for the period 1982–2008. *Glob. Chang. Biol.* **2011**, *17*, 2385–2399. [CrossRef]
17. Wu, C.; Chen, J.M.; Black, T.A.; Price, D.T.; Kurz, W.A.; Desai, A.R.; Gonsamo, A.; Jassal, R.S.; Gough, C.M.; Bohrer, G.; et al. Interannual variability of net ecosystem productivity in forests is explained by carbon flux phenology in autumn. *Global Ecol. Biogeogr.* **2013**, *22*, 994–1006. [CrossRef]
18. Lee, S.; Jeong, S.; Park, C.E.; Kim, J. A Simple method of predicting autumn leaf coloring date using machine learning with spring leaf unfolding date. *Asia-Pac. J. Atmos. Sci.* **2022**, *58*, 219–226. [CrossRef]
19. Menzel, A.; Sparks, T.H.; Estrella, N.; Koch, E.; Aasa, A.; Ahas, R.; Alm-Kübler, K.; Bissolli, P.; Braslavská, O.; Briede, A.; et al. European phenological response to climate change matches the warming pattern. *Glob. Chang. Biol.* **2006**, *12*, 1969–1976. [CrossRef]
20. Lang, W.; Chen, X.; Qian, S.; Liu, G.; Piao, S. A new process-based model for predicting autumn phenology: How is leaf senescence controlled by photoperiod and temperature coupling? *Agric. For. Meteorol.* **2019**, *268*, 124–135. [CrossRef]
21. Chu, X.; Man, R.; Zhang, H.; Yuan, W.; Tao, J.; Dang, Q.L. Does climate warming favour early season species? *Front. Plant Sci.* **2021**, *12*, 765351. [CrossRef] [PubMed]
22. Chen, S.; Fu, Y.H.; Geng, X.; Hao, Z.; Tang, J.; Zhang, X.; Xu, Z.; Hao, F. Influences of shifted vegetation phenology on runoff across a hydroclimatic gradient. *Front. Plant Sci.* **2022**, *12*, 802664. [CrossRef] [PubMed]
23. Keskitalo, J.; Bergquist, G.; Gardestrom, P.; Jansson, S. A cellular timetable of autumn senescence. *Plant Physiol.* **2005**, *139*, 1635–1648. [CrossRef]
24. Saxe, H.; Cannell, M.G.R.; Johnsen, Ø.; Ryan, M.G.; Vourlitis, G. Tree and forest functioning in response to global warming. *New Phytol.* **2001**, *149*, 369–399. [CrossRef] [PubMed]
25. Estiarte, M.; Peñuelas, J. Alteration of the phenology of leaf senescence and fall in winter deciduous species by climate change: Effects on nutrient proficiency. *Glob. Chang. Biol.* **2015**, *21*, 1005–1017. [CrossRef] [PubMed]
26. Bucher, S.F.; Römermann, C.; Bonser, S. The timing of leaf senescence relates to flowering phenology and functional traits in 17 herbaceous species along elevational gradients. *J. Ecol.* **2021**, *109*, 1537–1548. [CrossRef]
27. Zani, D.; Crowther, T.W.; Mo, L.D.; Renner, S.S.; Zohner, C.M. Increased growing-season productivity drives earlier autumn leaf senescence in temperate trees. *Science* **2020**, *370*, 1066–1071. [CrossRef]
28. Xia, H.; Wang, B. Complete chloroplast genome sequence of the Mongolian oak, *Quercus mongolica* (Fagaceae). *Mitochondrial DNA Part B* **2019**, *4*, 1089–1090. [CrossRef]
29. Hu, M.X.; Zhou, G.S.; Lü, X.M.; Wang, S.Q.; Zhang, S.Y. Interactive effects of different warming and changing photoperiod on spring phenology of *Quercu smongolicus* seedlings. *Acta Ecol. Sin.* **2021**, *41*, 2816–2825. [CrossRef]
30. Wan, M.W.; Liu, X.Z. *Phenological Observation Methods in China*; Science Press: Beijing, China, 1979.
31. Davis, J.E.; Arkebauer, T.J.; Norman, J.M.; Brandle, J.R. Rapid field measurement of the assimilation rate versus internal CO_2 concentration relationship in green ash (*Fraxinus pennsylvanica* Marsh.): The influence of light intensity. *Tree Physiol.* **1987**, *3*, 387–392. [CrossRef]
32. McDermitt, D.; Norman, J.; Davis, J.; Ball, T.; Arkebauer, T.; Welles, J.; Roerner, S. CO_2 response curves can be measured with a field-portable closed-loop photosynthesis system. *Ann. Sc. For.* **1989**, *46*, 416s–420s. [CrossRef]
33. Zhou, H.; Zhou, G.; He, Q.; Zhou, L.; Ji, Y.; Lv, X. Capability of leaf water content and its threshold values in reflection of soil–plant water status in maize during prolonged drought. *Ecol. Indic.* **2021**, *124*, 107395. [CrossRef]
34. Garnier, E.; Laurent, G. Leaf anatomy, specific mass and water content in congeneric annual and perennial grass species. *New Phytol.* **1994**, *128*, 725–736. [CrossRef]
35. Fracheboud, Y.; Luquez, V.; Bjorken, L.; Sjodin, A.; Tuominen, H.; Jansson, S. The control of autumn senescence in European aspen. *Plant Physiol.* **2009**, *149*, 1982–1991. [CrossRef] [PubMed]
36. Inoue, S.; Dang, Q.L.; Man, R.; Tedla, B. Photoperiod, [CO_2] and soil moisture interactively affect phenology in trembling aspen: Implications to climate change-induced migration. *Environ. Exp. Bot.* **2020**, *180*, 104269. [CrossRef]
37. Estrella, N.; Menzel, A. Responses of leaf colouring in four deciduous tree species to climate and weather in Germany. *Clim. Res.* **2006**, *32*, 253–267. [CrossRef]
38. Delpierre, N.; Dufrêne, E.; Soudani, K.; Ulrich, E.; Cecchini, S.; Boé, J.; François, C. Modelling interannual and spatial variability of leaf senescence for three deciduous tree species in France. *Agric. For. Meteorol.* **2009**, *149*, 938–948. [CrossRef]
39. Singh, R.K.; Bhalerao, R.P.; Eriksson, M.E. Growing in time: Exploring the molecular mechanisms of tree growth. *Tree Physiol.* **2021**, *41*, 657–678. [CrossRef]
40. Meng, L.; Zhou, Y.; Gu, L.; Richardson, A.D.; Penuelas, J.; Fu, Y.; Wang, Y.; Asrar, G.R.; De Boeck, H.J.; Mao, J.; et al. Photoperiod decelerates the advance of spring phenology of six deciduous tree species under climate warming. *Glob. Chang. Biol.* **2021**, *27*, 2914–2927. [CrossRef]
41. Doi, H.; Takahashi, M. Latitudinal patterns in the phenological responses of leaf colouring and leaf fall to climate change in Japan. *Global Ecol. Biogeogr.* **2008**, *17*, 556–561. [CrossRef]
42. Fu, Y.H.; Piao, S.; Delpierre, N.; Hao, F.; Hanninen, H.; Liu, Y.; Sun, W.; Janssens, I.A.; Campioli, M. Larger temperature response of autumn leaf senescence than spring leaf-out phenology. *Glob. Chang. Biol.* **2018**, *24*, 2159–2168. [CrossRef] [PubMed]
43. Wang, G.; Huang, Y.; Wei, Y.; Zhang, W.; Li, T.; Zhang, Q. Inner Mongolian grassland plant phenological changes and their climatic drivers. *Sci. Total Environ.* **2019**, *683*, 1–8. [CrossRef] [PubMed]

44. Wu, L.; Ma, X.; Dou, X.; Zhu, J.; Zhao, C. Impacts of climate change on vegetation phenology and net primary productivity in arid Central Asia. *Sci. Total Environ.* **2021**, *796*, 149055. [CrossRef] [PubMed]
45. Gunderson, C.A.; Edwards, N.T.; Walker, A.V.; O'Hara, K.H.; Campion, C.M.; Hanson, P.J. Forest phenology and a warmer climate-growing season extension in relation to climatic provenance. *Glob. Chang. Biol.* **2012**, *18*, 2008–2025. [CrossRef]
46. Morin, X.; Roy, J.; Sonie, L.; Chuine, I. Changes in leaf phenology of three European oak species in response to experimental climate change. *New Phytol.* **2010**, *186*, 900–910. [CrossRef]
47. Pudas, E.; Tolvanen, A.; Poikolainen, J.; Sukuvaara, T.; Kubin, E. Timing of plant phenophases in Finnish Lapland in 1997–2006. *Boreal Environ. Res.* **2008**, *13*, 31–43.
48. Tanino, K.K.; Kalcsits, L.; Silim, S.; Kendall, E.; Gray, G.R. Temperature-driven plasticity in growth cessation and dormancy development in deciduous woody plants: A working hypothesis suggesting how molecular and cellular function is affected by temperature during dormancy induction. *Plant Mol. Biol.* **2010**, *73*, 49–65. [CrossRef]
49. Barr, A.G.; Black, T.A.; Hogg, E.H.; Kljun, N.; Morgenstern, K.; Nesic, Z. Inter-annual variability in the leaf area index of a boreal aspen-hazelnut forest in relation to net ecosystem production. *Agric. For. Meteorol.* **2004**, *126*, 237–255. [CrossRef]
50. Frechette, E.; Chang, C.Y.; Ensminger, I. Variation in the phenology of photosynthesis among eastern white pine provenances in response to warming. *Glob. Chang. Biol.* **2020**, *26*, 5217–5234. [CrossRef]
51. Kong, D.; Zhang, Y.; Wang, D.; Chen, J.; Gu, X. Photoperiod explains the asynchronization between vegetation carbon phenology and vegetation greenness phenology. *J. Geophys. Res. Biogeosci.* **2020**, *125*, 1–15. [CrossRef]
52. Bauerle, W.L.; Oren, R.; Way, D.A.; Qian, S.S.; Stoy, P.C.; Thornton, P.E.; Bowden, J.D.; Hoffman, F.M.; Reynolds, R.F. Photoperiodic regulation of the seasonal pattern of photosynthetic capacity and the implications for carbon cycling. *Proc. Natl. Acad. Sci. USA* **2012**, *109*, 8612–8617. [CrossRef] [PubMed]
53. Kinoshita, T.; Kume, A.; Hanba, Y.T. Seasonal variations in photosynthetic functions of the urban landscape tree species *Gingko biloba*: Photoperiod is a key trait. *Trees* **2020**, *35*, 273–285. [CrossRef]